J. Iran. Chem. Soc., Vol. 7, Suppl., July 2010, pp. S42-S51.

JOURNAL OF THE
Iranian
Chemical Society

Synthesis and Characterization of Hippurate-Layered Double Hydroxide Nanohybrid and Investigation of its Release Property

M.Z. Hussein[a,b,*], F.A. Bahar[a] and A. Hj Yahaya[c]

[a]*Advanced Material and Nanotechnology Laboratory, Institute of Advanced Technology (ITMA), Universiti Putra Malaysia, 43000 UPM, Serdang, Selangor Malaysia*

[b]*Department of Chemistry, Faculty of Science, Universiti Putra Malaysia, 43000 UPM, Serdang, Selangor Malaysia*

[c]*Centre of Foundation Studies for Agricultural Science, Universiti Putra Malaysia, 43000 UPM, Serdang, Selangor Malaysia*

(Received 6 November 2008, Accepted 23 April 2009)

The anion of hippuric acid, hippurate (A^-), as an organic guest was intercalated into the interlayers of anionic clay, Zn/Al hydrotalcite-like or layered double hydroxides (LDH) host by direct co-precipitation method from aqueous solution for the formation of new nanohybrid compounds, Zn/Al-hippurate nanohybrids (ZAHs). Various Zn/Al molar ratios (R) = 3-5 and concentrations of HA (0.06-0.15 M) were used for the synthesis. ZAHs synthesized, using 0.15 M HA, was found to give well-ordered layered nanohybrid materials with an increase of the basal spacing to 19.6-21.0 Å compared to 8.8-9.0 Å in the LDHs. The increase in the basal spacing is due to the insertion of A^- organic moiety into the LDH interlayers. Formation of the host-guest type of material was confirmed by XRD, FTIR, TGA/DTG and compositional analysis. The release of the intercalated guest was found to be tunable in a controlled manner by Zn/Al molar ratio and is governed by pseudo-second order kinetics. Thus, by varying the experimental conditions, the release property of the guest anion can be tailored as required.

Keywords: Anionic clay, Hippuric acid, Intercalation, Layered double hydroxides, Hydrotalcite, Nanohybrid

INTRODUCTION

Layered double hydroxides (LDHs), also known as hydrotalcite-like materials or anionic clays consist of a large group of natural and synthetic materials. They are formed when an appropriate combination of metal salts is exposed to a base. This leads to the formation of positively charged mixed metal hydroxide layers, which require exchangeable anions to counterbalance the positive charge [1]. The compound also contains various amounts of water, which is bonded to the hydroxide layer and/or to the interlayer anions, where the metal cations are octahedrally coordinated by hydroxide groups [2]. LDHs consist of brucite-like material, $Mg(OH)_2$. Each Mg^{2+} ion is octahedrally surrounded by six OH^- ions and different octahedral share edges to form an infinite two-dimensional layer. Divalent cations are partially iso-morphously replaced by trivalent cations giving positively charged layers with interlayer charge-compensating anionic species [3].

LDH can be represented by $[M^{2+}_{1-x}M^{3+}_{x}(OH)_2]A^{n-}_{x/n}.mH_2O$, where M^{2+} and M^{3+} are divalent and trivalent metal ions, respectively, A^{n-} is the interlayer anions and x as the $M^{2+}/[M^{2+} + M^{3+}]$, *i.e.* the mole fraction of M^{2+} in the inorganic brucite layers.

*Corresponding author. E-mail: mzobir@putra.upm.edu.my

Among the applications of LDHs are: adsorbents for the removal of organic and inorganic pollutants from water, ion-exchangers, catalyst precursors, and in pharmaceuticals for drug release and delivery [2,4-8]. This is due to the property of LDHs, which have high anionic capacity compared to cationic clays such as smectite and vermiculite [9].

Co-precipitation method is one among many others adopted by many researchers to synthesize LDHs and their nanohybrids due to the presence of homogeneous starting materials [10]. Synthesis of LDHs with anions such as NO_3^- and Cl^- as counter anions has received great attention in recent years because of their large anion-exchange capacity [10-11]. Previous studies show that pH plays an important role in determining the resulting properties of Zn/Al-LDH and the exchange of nitrate by phosphate ions [12]. The anion exchange property was also observed when chromate was incorporated into LDHs to study their possible uses as chromate scavenging agents for green chemistry applications [13]. In addition, various ratios of the cations used, namely (M^{2+} = Mg, Cd, Co, Zn and Fe; M^{3+} = Al, Cr, Ga and Mn) have been previously studied to determine their effect on the formation of nanohybrids [7,14-15].

A variety of anionic species can be intercalated into the interlayer of LDHs and the interlayer will expand to accommodate the bulky size of the guest. The formation of the so-called nanohybrid or nanocomposite materials can be accomplished by using different organic moieties [5] and different routes of synthesis [4,16].

The objective of this study is to use Zn-Al-hydrotalcite-like synthetic mineral, as an inorganic host for the formation of well-ordered, phase-pure 2D layered nanohybrid material by intercalation of A^- into the mineral host using direct co-precipitation method. The resulting material is subsequently used as a controlled release formulation by studying its release property.

EXPERIMENTAL

Chemicals

The chemicals used in this study were aluminum nitrate nanohydrate ($Al(NO_3)_3.9H_2O$, HMBG), zinc nitrate tetrahydrate ($Zn(NO_3)_2.4H_2O$, MERCK), sodium hydroxide (NaOH, SYSTERM), hippuric acid (HA) ($C_9H_9NO_3$, ACROS) and anhydrous sodium carbonate (Na_2CO_3, HMBG). All chemicals were used without any purification. Purified nitrogen gas was used for the N_2 atmosphere to avoid carbonate (CO_3^{2-}) contamination due to the absorption of CO_2 from the air.

Synthesis of the LDH and Its Nanohybrid

Direct co-precipitation method was used to intercalate A^- into the interlayer of LDH. All experiments were done under N_2 flow to avoid the contamination by atmospheric CO_2. The HA solution was added into a solution containing $Zn(NO_3)_2$ and $Al(NO_3)_3$ with different Zn/Al molar ratios, R, of 3, 4 and 5 with vigorous stirring. The resulting solution was adjusted to pH 7.5 by simultaneous addition of 1.0 M NaOH solution. Various concentrations of HA were used for the synthesis, including 0.06, 0.08, 0.10 and 0.15 M. The resulting solution was aged for 18 h in an oil bath shaker at 70 °C, filtered, washed and dried in an oven at 65 °C for 2 days. A similar method was used to prepare Zn/Al-LDH with nitrate as the intergallery anion (LDH) by omitting the addition of HA solution into the mother liquid.

Characterizations

The resulting materials were characterized by a powder x-ray diffractometer (Ital Structure APD 2000) and a Fourier transform infrared spectrometer (FTIR) model Thermo Nicolet Nexus, using KBr pellet technique in the range of 400-4000 cm^{-1} with a resolution of 4 cm^{-1}. The surface characterization of the samples was carried out by adsorption-desorption of nitrogen gas at liquid nitrogen temperature (77 K), using a Micromeritics ASAP 2000 instrument. Inductively coupled plasma-atomic emission spectroscopy (ICP-AES), using a Perkin Elmer Spectrophotometer model Optima 2000DV and CHNS Analyzer model CHNS-932 (LECO) were used to analyze the chemical composition of the samples. Thermogravimetric and differential thermogravimetric analyses (TGA/DTG) were carried out using a Mettler Toledo TGA/SDTA851 thermogravimetric analyzer with heating rate of 10 °C min^{-1} between 35-1000 °C, under nitrogen flow rate of about 50 ml min^{-1}. The morphology of the samples was observed using a JEOL JSM-6400 Scanning Electron Microscope (SEM).

Controlled Release Study

Release of A^- from the nanohybrid was investigated by

adding 0.6 mg of ZAHs synthesized at R = 3, 4 and 5 into 3.5 ml of aqueous 0.0025 M Na_2CO_3 solution. The accumulated amount of A^- released into the solution was measured at preset times using a Perkin Elmer UV-Vis Spectrophotometer model Lambda 35.

RESULTS AND DISCUSSION

Powder X-Ray Diffraction

Figure 1 shows the powder x-ray diffraction (XRD) patterns of ZAHs and LDHs that were synthesized at Zn/Al molar ratio, R = 3, 4 and 5 using 0.06, 0.08, 0.10 and 0.15 M HA at pH 7.5. Molecular structure of HA is given in the inset of Fig. 1. The XRD patterns show typical features of LDH and its intercalated compound, with sharp and intense reflection at low 2θ angle and less intense reflection at higher angular values [2]. Noteworthy also is that the intensity of the 003 reflection of the nanohybrid generally increased as the concentration of the HA increased, and at the same time the ZnO phase gradually decreased. This shows that a mixed phase was transformed to a pure phase due to the complete intercalation of the A^- into the LDH interlayers and this was achieved for all Rs values at 0.15 M HA. These materials were subsequently used for further characterizations (Fig. 2). In addition, LDHs synthesised at the same Rs were also chosen for comparison. As shown in Fig. 1, the basal spacing for LDH synthesized at R = 3, 4 and 5 is 8.8 Å, 9.0 Å and 8.8 Å, respectively, which is comparable to the value obtained previously [3]. The d-spacing for ZAHs prepared at R = 3, 4 and 5 is 19.6, 21.0 and 21.0 Å, respectively. The increase in basal spacing for ZAH in comparison with their corresponding LDH is due to the insertion of A^- which is bulkier than nitrate together with the spatial orientation of A^- into the LDH interlayers.

Fourier Transform Infrared Spectra

Fourier transform infrared (FTIR) is used to identify the existence of the guest anion (A^-) in the interlayer of the LDH.

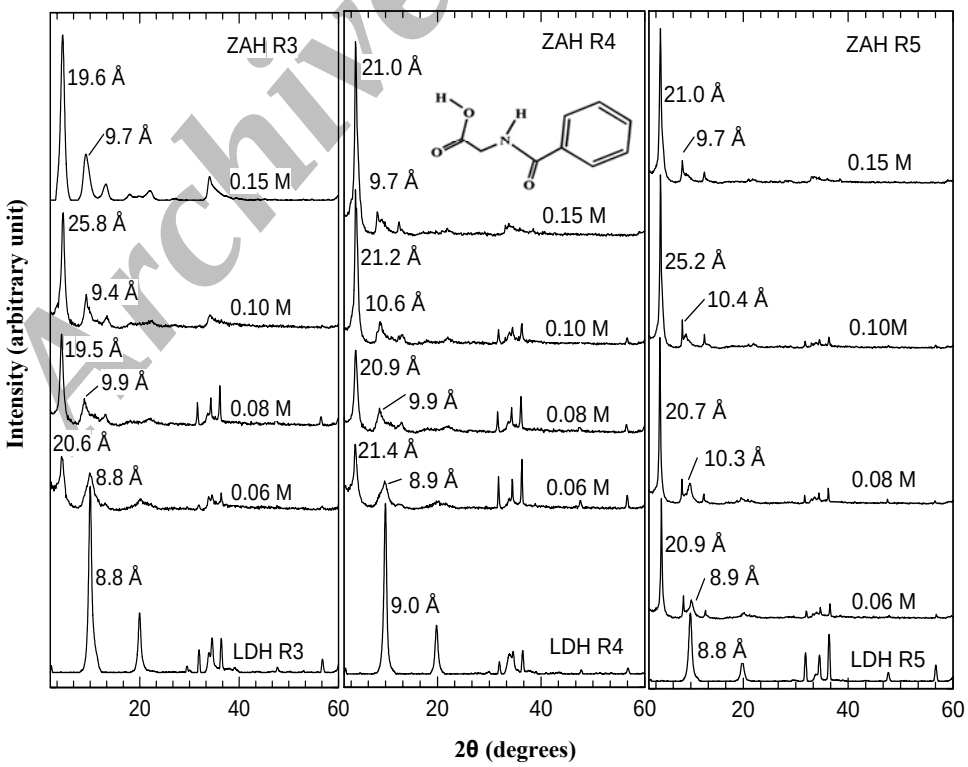

Fig. 1. XRD patterns of ZAHs synthesized at R = 3, 4 and 5 and 0.06-0.15 M hippuric acid at pH 7.5. Molecular structure of hippuric acid is shown in the inset.

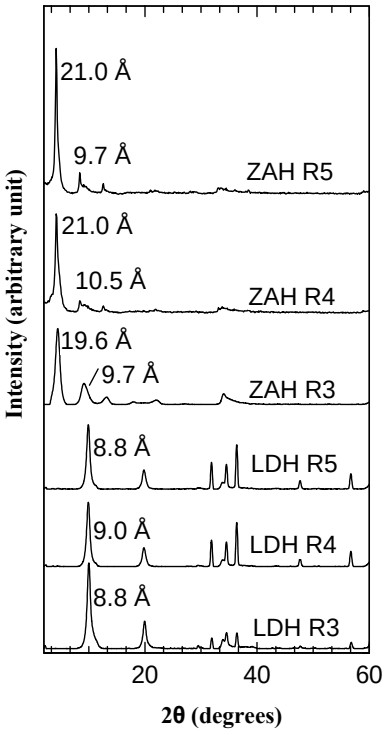

Fig. 2. XRD patterns of LDHs and ZAHs synthesized at R = 3, 4 and 5 using 0.15 M hippuric acid at pH 7.5.

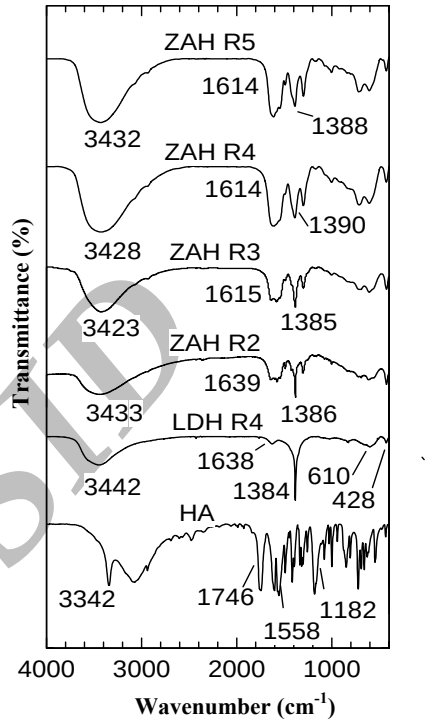

Fig. 3. FTIR spectra of hippuric acid, LDH R4 and ZAHs synthesized at R = 3, 4, 5 using 0.15 M hippuric acid at pH 7.5

Figure 3 shows the FTIR spectra for HA, LDH and ZAH synthesized at R = 3, 4 and 5. The FTIR spectrum for LDH shows absorption band at 3442 cm^{-1} which can be attributed to OH group of the LDH. A shoulder observed at around 3000 cm^{-1}; is due to the hydrogen bonding between H_2O and the anion in the interlayer [2]. A sharp and intense absorption band at 1384 cm^{-1}, and a less intense absorption band at 1633 cm^{-1} are due to the respective symmetric and asymmetric stretching of the NO_3^- group. A weak band at around 600 cm^{-1} can be attributed to the metal-oxygen bond stretching modes in the LDH sheets [4,12]. The FTIR spectrum of HA exhibits a band at 3342 cm^{-1}, indicating the presence of N-H stretching. The bands at around 1500 cm^{-1} are due to the stretching vibration of aromatic ring, C=C, and absorption band at 1746 cm^{-1} is due to C=O stretching in the HA [17]. Figure 3 also shows the FTIR spectra of ZAHs synthesized at R = 3, 4 and 5. These spectra show the combined spectral features of both the HA and LDH, confirming the presence of both functional groups of HA and LDH in ZAH. This verifies the encapsulation of A^- in the interlayer of LDH for the formation of a new host-guest type of material.

Surface Properties

Adsorption-desorption isotherm and surface area

Figure 4 shows the nitrogen adsorption-desorption isotherms of LDH, and ZAHs synthesized at R = 3, 4 and 5. All the adsorption isotherms are of Type IV indicating mesoporous type material (20-500 Å) [18]. The Type IV characteristics were observed with adsorption increasing slowly at low relative pressure in a range of 0.0-0.8, followed by rapid adsorption at relative pressure >0.8. For both LDHs and ZAHs, the maximum volume adsorbed increased when the R value increased. For the ZAHs synthesized at R = 4 and 5, the optimum uptake is higher than their corresponding LDHs, while for the LDHs synthesised at R = 3, the optimum uptake is lower than LDH. ZAHs synthesised at R = 4 and 5 show the desorption branch of the hysteresis loop which is wider than

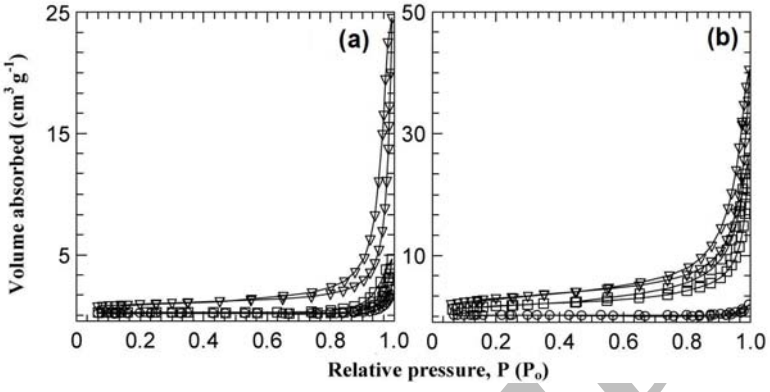

Fig. 4. Nitrogen adsorption-desorption isotherms: (a) LDHs (▽, LDH R5; □, LDH R4; ○, LDH R3), (b) ZAHs (▽, ZAH R5; □, ZAH R4; ○, ZAH R3). R = 3, 4 and 5 using 0.15 M hippuric acid at pH 7.5.

LDH indicating different pore texture of the resulting materials. This is suggested to be due to modification of the pores as a result of the expansion of the basal spacing together with the formation of the new nanohybrid [3]. Figure 4 shows that the volume absorbed increases with the Zn/Al molar ratio, R. Table 1 shows the BET surface area of the LDHs and their nanohybrids, ZAHs. As shown in Table 1, except for R = 3, the surface area of the resulting nanohybrids is generally higher than their corresponding LDHs. For both of them, the BET surface area increased as the R values increased, except for the LDH synthesized at R = 3 in which the surface area decreased from 11.1 to 0.9 m^2 g^{-1}. The surface area of LDHs and ZAHs is in the range 0.9-3.4 and 0.9-11.1 m^2 g^{-1}, respectively.

Pore size distribution. The BJH pore size distributions for LDHs and ZAHs synthesized at R = 3, 4 and 5, as shown in Fig. 5, indicate that all the materials are of mesoporous-type. For both the LDHs and ZAHs, the pore volume generally increased as the R values increased. The BJH pore size distribution for LDH and ZAH synthesized at R = 5 shows an intense peak around 500 and 700 Å, compared to those synthesized at R = 4, which show less intense broad peaks at around 350 and 450 Å for LDH and ZAH, respectively. The intensity of the samples became less pronounced as the R value decreased to R = 3. The difference in peak values and pore volume values in the pore size distribution of LDHs and ZAHs indicate the modification of the pore texture which occurred when intercalation of A^- took place, in agreement with the formation of nanohybrids when A^- was intercalated inside the LDH [4,19].

The BJH average pore diameter and pore volume (Table 1) show a general increase with increasing R for both LDHs and their nanohybrids. However, the pore diameter was found to decrease when the HA^- was intercalated into the LDH interlayers for the formation of the ZAHs nanohybrids from 196-145, 280-167 and 330-179 Å for R of 3, 4 and 5, respectively. The desorption pore volume also decreases from 1.3 cm^3 g^{-1} for LDH to 0.6 cm^3 g^{-1} for ZAH at R = 3. However, for R of 4 and 5, the pore volumes of ZAH increase from 0.8 - 8.7 and 4.2-13.0, respectively, with respect to the corresponding LDH.

Compositional Analysis

The organic and inorganic compositions of all the samples are compared in Table 1. The resulting R values for the synthesized LDHs are 2.9, 3.7 and 4.4, compared to the starting values of 3, 4 and 5 in the mother liquids, respectively. The corresponding final R values obtained for ZAHs are 2.7, 3.7 and 4.6, respectively. For both the LDHs and ZAHs, a slightly lower R value than the original ones indicate that less Al^{3+} ions are actually present in the resulting nanohybrids. The value of mole fraction of Al^{3+} in the inorganic brucite-like layers (x_{Al}) also decreased with the increasing of the Zn/Al molar ratio as shown in Table 1.

The presence of nitrogen in LDHs and ZAHs synthesized at R = 3, 4 and 5 obtained from CHNS analysis (Table 1)

Table 1. Physicochemical Properties of LDHs and Their Corresponding Nanohybrids, ZAHs Synthesized at Various Zn/Al Molar Ratios at pH 7.5

R_i	BS (Å)	BET-SA (m^2g^{-1})	BJH-DPV (cm^3g^{-1})	BJH-APD (Å)	R_f	C (%)	N (%)	X_{Al}	Ideal formula	Thermal properties: Temperature range (°C) 25-200	201-300	300-600	601-1000	TWL (%)
									LDHs					
3	8.8	1.1	1.3	196	2.9	-	3.1	0.26	$[Zn_{0.74}Al_{0.26}(OH)_2][NO_3^-]_{0.26}.0.43H_2O$	6.90	15.89	12.48	2.76	38.03
4	9.0	0.9	0.8	280	3.7	-	3.5	0.21	$[Zn_{0.79}Al_{0.21}(OH)_2][NO_3^-]_{0.21}.0.24H_2O$	3.92	28.10	-	-	32.02
5	8.8	3.4	4.2	330	4.4	-	2.6	0.18	$[Zn_{0.82}Al_{0.18}(OH)_2][NO_3^-]_{0.18}.0.21H_2O$	3.60	12.60	10.39	-	26.59
									Nanohybrids (ZAHs)					
3	19.6	0.9	0.6	145	2.7	23.0(57.3)	2.9	0.27	$[Zn_{0.73}Al_{0.27}(OH)_2][HA]_{0.27}.0.63H_2O$	7.60	12.72	28.13	4.60	53.05
4	21.0	6.4	8.7	167	3.7	24.1(60.3)	2.8	0.21	$[Zn_{0.79}Al_{0.21}(OH)_2][HA]_{0.21}.0.24H_2O$	3.33	1.85	33.00	19.00	57.18
5	21.0	11.1	13.0	179	4.6	22.5(55.9)	2.4	0.18	$[Zn_{0.82}Al_{0.18}(OH)_2][HA]_{0.18}.0.43H_2O$	5.80	2.43	25.80	12.4	46.43

R_i = Initial Zn/Al ratio; R_f = Final Zn/Al ratio; BS = Basal spacing; BET-SA = BET surface area; BJH-DPV = BJH desorption pore volume; BJH-APD = BJH average pore diameter; C = Loading of HA; TWL = Total weight loss.

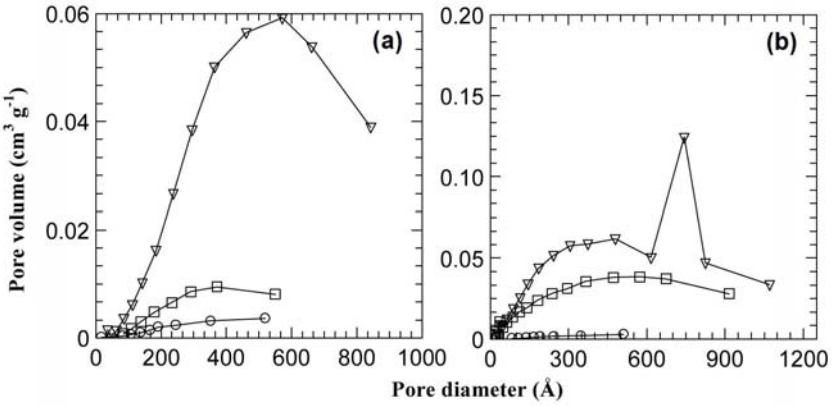

Fig. 5. BJH pore size distributions for LDHs (a) and ZAHs (b) synthesized at R = 3, 4 and 5 using 0.15 M hippuric acid at pH 7.5: (a) LDHs (▽, LDH R5; □, LDH R4; ○, LDH R3), (b) ZAHs (▽, ZAH R5; □, ZAH R4; ○, ZAH R3).

indicates the presence of nitrate and A^- in LDHs and ZAHs, respectively. However, the presence of nitrate in the ZAHs, as shown by a sharp absorption band at around 1385 cm^{-1} in the FTIR spectrum (Fig. 3), can not be ruled out. This can be due to co-intercalation and/or adsorbed species of nitrate in the resulting nanohybrid materials. The percentage loading of the hippurate anion estimated from the percentage value of carbon obtained from CHNS analysis, were found to be 57.3, 60.3 and 55.9% for the ZAHs synthesized at R = 3, 4 and 5, respectively.

Thermal Analysis

Figure 6 shows the TGA and DTG curves of the samples which can be divided into three stages; (1) removal of physisorbed water from the surface and hydroxide inter layers, (2) dehydroxylation of the hydroxide layers and (3) elimination and combustion of the organic anion (A^-). Stage 2 and 3 usually overlap [5]. The range of the temperature is determined by the nature of the metal anions, M^{2+} and M^{3+} [1]. The results are summarized in Table 1.

TGA-DTG thermograms of LDHs and ZAHs synthesized at R = 3, 4 and 5 (Fig. 6) indicate the removal of water physisorbed on the external surface and between the hydroxides layers well below 200 °C. For LDHs, dehydroxylation of the hydroxides layers occurred between 220-600 °C and the nitrate anions are completely removed approximately at or higher than 650 °C.

For ZAHs synthesized at R = 3, 4 and 5, dehydroxylation of the hydroxide layers and the elimination and combustion of the HA^- may have overlapped and occurred in the range 300-500 °C [10] with the weight loss of 28.10, 33.00 and 25.80%, respectively as shown in Table 1. Only metal oxides remain after 600 °C. This shows that A^- was thermally more stable when it was intercalated into the inorganic LDH host compared to the bare one. The results of the compositional and thermal analyses were used to obtain chemical formulae for the LDHs and ZAHs (Table 1).

Surface Morphology

Figure 7 shows the surface morphology of LDH and ZAH

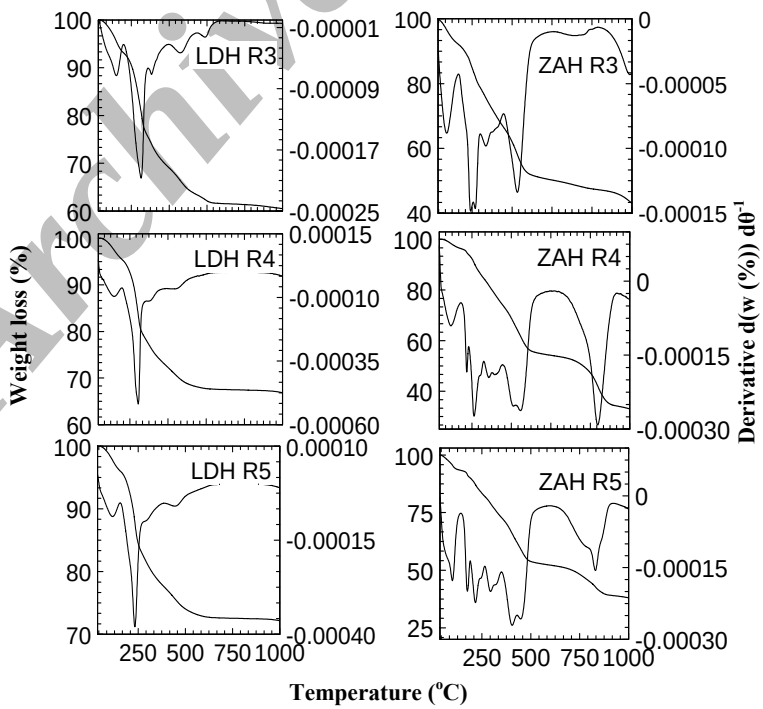

Fig. 6. TGA/DTG thermograms for LDHs and ZAHs synthesized at R = 3, 4, 5 using 0.15 M hippuric acid at pH 7.5.

obtained by SEM. Both images show typical morphology of the LDHs and ZAHs (Table 1). LDH and its intercalated compound, indicating the existence of the agglomerates of compact and non-porous granule structure. As shown in Fig. 7, there is no significant difference between the morphology of the LDH and ZAH and that of Zn-Al-24D nanocomposite and its LDH studied by Hussein *et al*. [20].

Kinetic Release

The release profiles of A^- into 0.0025 M Na_2CO_3 aqueous solution from the interlayer of ZAHs synthesized at R = 3, 4 and 5 during 0-800 min is shown in Fig. 8. The release rate of A^- from ZAH synthesized at R = 5 was found to be the most rapid compared to those synthesized at R = 3 and 4. The release of accumulated HA^- at saturated level was achieved at around 100 min for R = 5 and at around 400 min for both R = 3 and 4. The release profiles of the nanohybrids show that the percentage release of A^- decreases with the increase of Zn/Al molar ratio, R.

The data for the A^- release from the nanohybrids into aqueous carbonate solution were fitted into various models. The resulting parameters and the plots obtained are shown in Table 2 and Fig. 9, respectively. As shown in the table, the correlation coefficient (r^2) values for pseudo-second order kinetic equation was found to give the best fit compared to the other models used in this work for all the nanohybrids. As a result, the time taken for A^- concentration to increase to half of its initial values ($t_{1/2}$), are compared in Table 2.

The value of $t_{1/2}$ increases as the x_{Al} value increases. This can be explained by the fact that when the x_{Al} increases, then the inorganic LDH layers become more positively charged and therefore the electrostatic interactions between the host and the guest become stronger. As a result, release of the guest becomes more difficult. Similar trend can be observed for the release of the saturated percentage, and therefore, a similar explanation can be offered.

CONCLUSIONS

A new host-guest type nanohybrid material has been successfully synthesized by hybridization of hippurate moiety as the organic guest into the interlayer of anionic clay or hydrotalcite-like mineral host. Factors such as concentrations

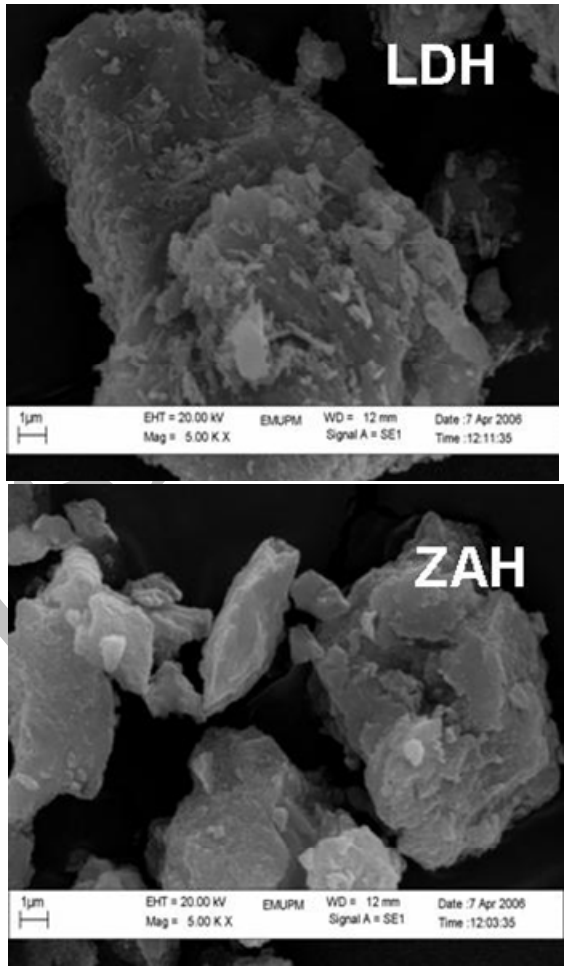

Fig. 7. SEM micrographs for LDH and ZAH at 5000x.

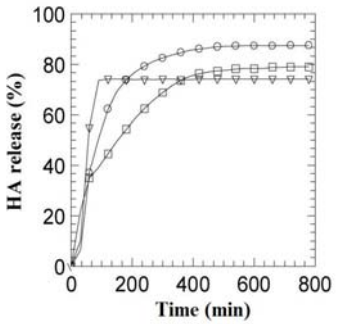

Fig. 8. Release profiles of HA into 0.0025 M Na_2CO_3 aqueous solution from ZAHs synthesized at R = 3, 4 and 5 using 0.15 M hippuric acid at pH 7.5: ○, ZAH R3; □, ZAH R4; ▽, ZAH R5.

Table 2. Percentage Release, Rate Constants (k), Half Life ($t_{1/2}$) and Correlation Coefficients (r^2) Obtained from Fitting of the Release Data of HA^- from ZAHs Nanohybrids Synthesized at R = 3, 4 and 5 into 0.0025 M Na_2CO_3 Aqueous Solution

		r^2				Other parameters for pseudo-second order	
ZAHs (R)	Saturated percentage release (%)	Zeroth order	First order	Parabolic diffusion model	Pseudo-second order	k (10^{-4}) (M min^{-1})	$t_{1/2}$ (min)
3	84.35	0.91	0.98	0.97	0.91	2.02	110
4	79.10	0.70	0.83	0.89	0.99	2.56	78
5	74.29	0.26	0.28	0.28	0.98	9.07	23

[a]Kinetic equations

Zeroth order	First order	Pseudo second order	Parabolic diffusion
$x = kt + c$	$-\log(1-x) = kt + c$	$t/M_i = 1/k_2M_f^2 + (1/M_f)t$	$M_i/M_f = kt^{0.5} + c$

[a]x is the percentage release of hippurate, HA^- at time, t (min) and c is a constant. k, M_i and M_f is the rate constant, the initial and final concentration of hippurate, respectively.

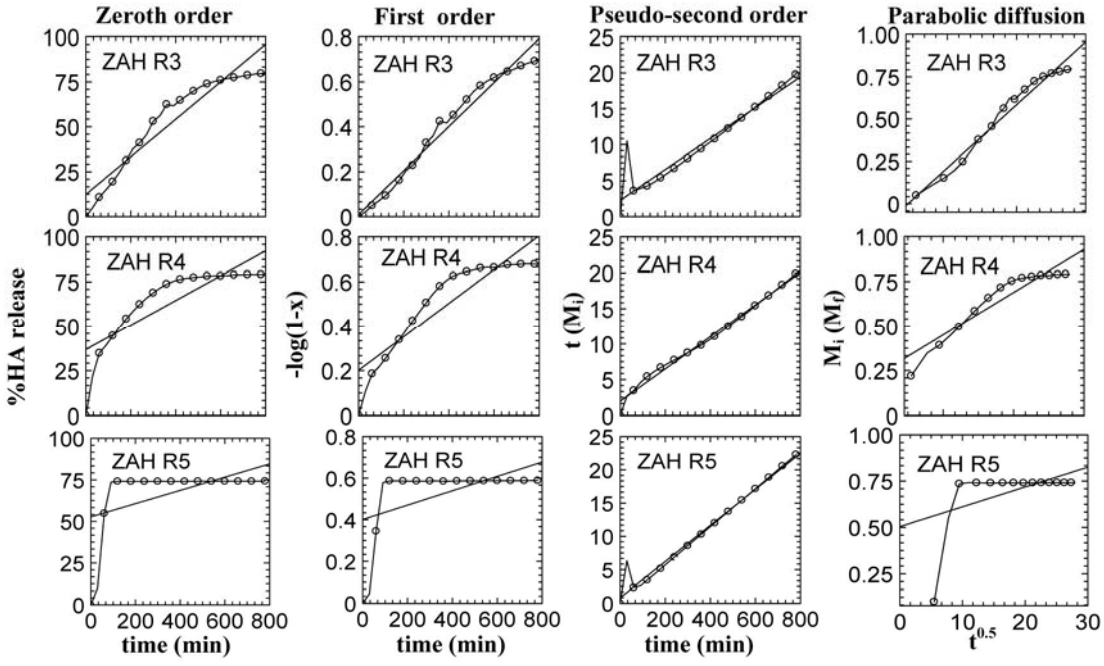

Fig. 9. Fitting of HA release data using zeroth-, first- and pseudo-second-order kinetics, and parabolic diffusion equations for ZAHs nanohybrids synthesized at R = 3, 4 and 5 using 0.15 M hippuric acid at pH 7.5.

and the Zn/Al molar ratio were important parameters to be optimized in order to get a well-ordered, phase-pure layered nanohybrid material. In addition, the Zn/Al molar ratio controlled the surface properties of the resulting LDH and the nanohybrid. Based on the increase of basal spacing, FTIR, TGA/DTG and compositional analyses, it is clear that the hippurate moiety was actually intercalated into the interlamellae of the host, brucite interlayers, for the formation of new nanohybrid compounds. The release study indicates that hippurate-intercalated LDHs show a controlled release property, where the guest anion, hippurate, can be ion exchanged in aqueous Na_2CO_3 solution. The kinetics and the ion exchange process were found to be dependent on the Zn/Al mole ratio and this can be used to tailor the release property of the guest anion.

ACKNOWLEDGMENTS

Financial support for this research was provided by the Ministry of Science, Technology and Innovation of Malaysia (MOSTI), under the IRPA Grant No. 09-02-04-0897-EAR001. FAB would like to thank Universiti Putra Malaysia for GRA.

REFERENCES

[1] S.P. Newman, W. Jones, New J. Chem. 22 (1998) 105.
[2] F. Cavani, F. Trifiro, A. Vaccari, Catal. Today 11 (1991) 173.
[3] M.Z.B. Hussein, K.H. Tan, J. Nanopart. Res. 2 (2000) 293.
[4] S. Miyata, Clays Clay Miner. 23 (1975) 369.
[5] V. Rives, Mater. Chem. Phys. 75 (2002) 19.
[6] S. Kwak, W.M. Kriven, M.A. Wallig, J. Chow, Biomaterials 25 (2004) 5995.
[7] A. Legrouri, M. Lakraimi, A. Barroug, A. De Roy, J.P. Besse, Water Res. 39 (2005) 3441.
[8] M. Lakraimi, A. Legrouri, A. Barroug, A. De Roy, J.P. Besse, Mater. Res. Bull. 41 (2006) 1763.
[9] J. Ortman, H.Y. Zhu, G.-Q. Lu, Sep. Purif. Technol. 31 (2003) 53.
[10] E.M. Seftel, E. Popovici, M. Mertens, K.D. Witte, G.V. Tendeloo, P. Cool, E.F. Vanstant, Micropor. Mesopor. Mat. 113 (2008) 296.
[11] S. Velu, V. Ramkumar, A. Narayanan, C.S. Swamy, J. Mater. Sci. 32 (1997) 957.
[12] A. Legrouri, M. Badreddine, A. Barroug, A. De Roy, J.P. Besse, J. Mater. Sci. Lett. 18 (1999) 1077.
[13] S.V. Prasanna, P.V. Kamath, C. Shivakumara, Mater. Res. Bull. 42 (2007) 1028.
[14] K. Zou, H. Zhang, X. Duan, Chem. Eng. Sci. 62 (2007) 2022.
[15] J. Inacio, C. Taviot-Gueho, C. Forano, J.P. Besse, Appl. Clay Sci. 18 (2001) 255.
[16] W.T. Reichle, Solid States Ionics 22 (1986) 135.
[17] D.L. Pavia, G.M. Lampman, G.S. Kriz, Introduction to Spectroscopy, 3rd ed., Brooks/Cole Thomson Learning, Inc., 2001.
[18] K.S.W. Sing, Colloids Surfaces 38 (1989) 113.
[19] M.Z.B. Hussein, Z.B. Jubri, Z. Zainal, A.H. Yahya, Mater. Sci.-Poland 22 (2004) 57.
[20] M.Z.B. Hussein, A.H. Yahya, Z. Zainal, H.K. Loo, Sci. Technol. Adv.